

MAGNETIC AND MORPHOLOGY CHARACTERIZATION OF NiZn FERRITE PREPARED FROM NANO SIZE STARTING POWDER VIA COPRECIPITATION TECHNIQUE

¹Tania Jahanbin and ²Mansor Hashim

¹*Department of Physics, Faculty of Science, Universiti Putra Malaysia,
43400 UPM Serdang, Selangor, Malaysia*

²*Institute of Advanced Technology (ITMA), University Putra Malaysia,
43400 UPM Serdang, Selangor, Malaysia*

ABSTRACT

Nanocrystalline nickel zinc ferrite of composition $\text{Ni}_{0.8}\text{Zn}_{0.2}\text{Fe}_2\text{O}_4$ has been synthesized by co precipitation technique. The as-dried powder was pressed into the toroid and pellet forms, then sintering them at sintering temperatures of 1100, 1200 and 1300°C. Then the samples were characterized by X-ray diffraction (XRD), initial permeability and relative loss factor. The physical properties such as bulk density and porosity were also studied. The density increased with sintering temperature. The highest density obtained was 4.48g/cm^3 . The initial permeability values were in the range of 10 -17 due to the small particle size. The relative loss factor was in the order of 10^{-3} - 10^{-5} in the frequency range of 1MHz to 1GHz. The results obtained gave better values than those obtained for ferrites prepared by conventional methods. The low loss makes these ferrites useful as inductor and transformer materials for high frequency applications.

INTRODUCTION

Nickel zinc ferrite is the most popular composition of soft ferrites. Due to the high resistivity and low eddy current losses and coercivity, these ferrites are used in high frequency applications as a core material for power transformers and circuit inductors in the megahertz frequency region. They are more stable, easily manufactured, and low cost and excellent magnetic properties. However, most ferrites have been produced via conventional methods with high temperature treatment. In the recent past, the wet methods have been found to have distinct advantages over the conventional dry processing [1, 2]. The wet methods are those such as sol-gel techniques, reverse micelles, host template, chemical coprecipitation, microemulsion procedures, precursor techniques, microwave plasma and mechanical milling for the fabrication of stoichiometric and chemically pure ferrite nanoparticles [3-12]. The co-precipitation method is widely used for preparation of ferrites due to its overriding advantages such as composition flexibility, economical, time saving and results in superior properties of ferrites processed at a much lower temperature [13].

The properties of Ni-Zn ferrites strongly depend on the method of preparation and heat treatment. The present work reports the magnetic properties, such as initial permeability and relative loss factor (RLF) of Ni-Zn ferrites prepared by the co precipitation technique and sintered at various temperatures.

EXPERIMENTAL

Synthesis

The starting materials used in the preparation of the selected composition $\text{Ni}_{0.8}\text{Zn}_{0.2}\text{Fe}_2\text{O}_4$ were nickel nitrate (98%), zinc nitrate (98%), ferric nitrate (98%) and ammonia hydroxide(25%) . Ammonia Hydroxide was used as a base because its salts are volatile on subsequent heating and hence impurity of the isolated powders due to the precipitating reagent can be avoided. In order to obtain the desired compositions, stoichiometric amounts of $\text{Ni}(\text{NO}_3)_2 \cdot 6\text{H}_2\text{O}$, $\text{Zn}(\text{NO}_3)_2 \cdot 6\text{H}_2\text{O}$ and $\text{Fe}(\text{NO}_3)_3 \cdot 9\text{H}_2\text{O}$ were dissolved in ultra-pure water. The solution of (100 ml of 0.08M $\text{Ni}(\text{NO}_3)_2 \cdot 6\text{H}_2\text{O}$, 100 ml of 0.2M $\text{Fe}(\text{NO}_3)_3 \cdot 9\text{H}_2\text{O}$, 100ml of 0.02M $\text{Zn}(\text{NO}_3)_2 \cdot 6\text{H}_2\text{O}$) were dissolved in distilled water with a constant stirring.

The precipitating reagent was added drop-wise into metal solutions, contained in a beaker, with constant stirring until co-precipitation occurred and the PH reached 10. The reaction temperature was kept at 85 °C for 45 min. The product was dried in an electric oven at a temperature of 110 °C for overnight to remove water contents. The dried powder was mixed homogeneously in a cleaned agate mortar and pestle. The powder was shaped into pellets and toroids using moulds and a hydraulic press. A load of 60 kN for 5 min was applied on each pellet and toroid .Then sintering at different temperatures was carried out.

Characterization

The structure and crystalline size were determined from the X-ray diffraction (XRD) data. XRD data were taken at room temperature using Cu $K\alpha$ ($\lambda=1.5406\text{\AA}$) radiation. The SEM photomicrographs were also taken to reveal the crystallization behaviour . The grain size was measured by the linear intercept method from SEM photographs. The Archimedes principle was used to determine the density of the sintered toroids. Both the initial permeability, μ_i and loss factor RLF were evaluated using the Agilent Impedance Analyzer model 4291B in the frequency range 1MHz-1GHz on the toroidal ferrite.

RESULTS AND DISCUSSION

The XRD analysis of the as- dried and samples calcined at different temperatures of 1100, 1200 and 1300°C for 5 hours are shown in Fig1. It confirms that the nickel zinc ferrite has the single phase cubic spinel structure and all the peaks observed matched well with the reflections of the nickel zinc ferrite reported in the standard card.

Table 1 shows the density and porosity of the Ni-Zn ferrite of composition $\text{Ni}_{0.8}\text{Zn}_{0.2}\text{Fe}_2\text{O}_4$ prepared by the coprecipitation method and sintered at various temperatures. It is observed that the density increases and porosity decreases with sintering temperature. The small amount of zinc evaporation at high temperature does not affect the density of ferrite. During sintering the grain growth increases may cause removing of the pores .Thus, density increases with higher sintering temperatures.

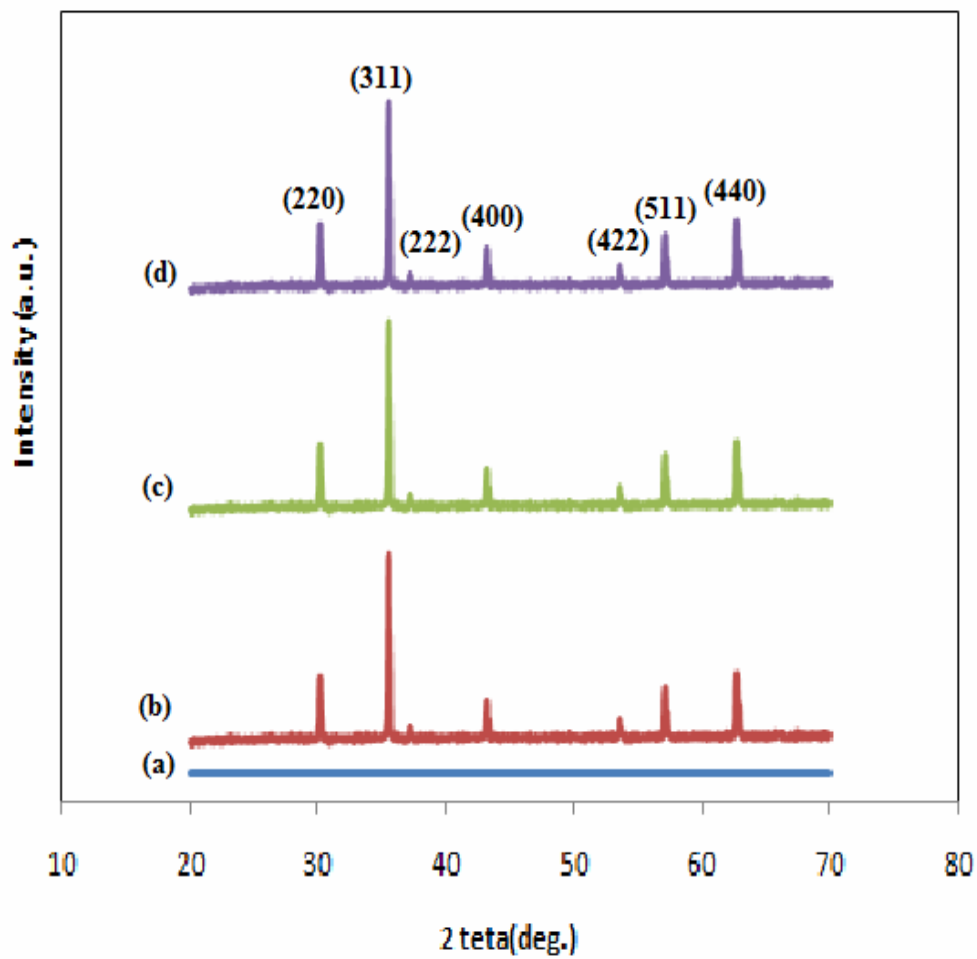


Figure 1: X-ray diffraction pattern of Ni_{0.8}Zn_{0.2}Fe₂O₄ Sintered at air, (b) 1100,(c)1200 ,(d)1300°C and (a) as dried in oven

Table1: Bulk density and porosity of Ni_{0.8}Zn_{0.2}Fe₂O₄ sintered at different temperatures

Sintering temperature(°C)	Bulk density (g.cm ⁻³)	Porosity (%)
1100	4.29	19
1200	4.372	18
1300	4.48	16

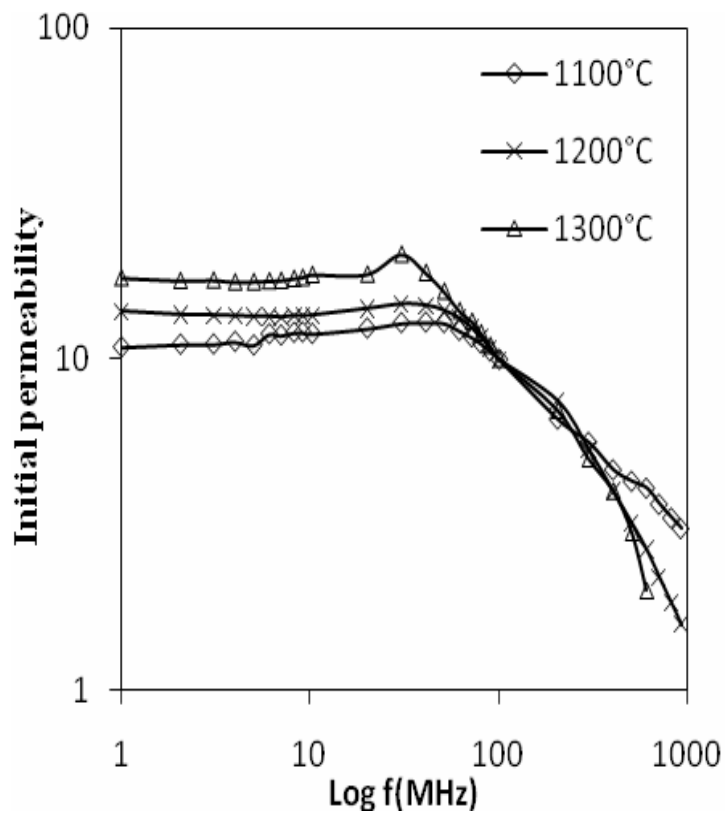


Figure 2: Variation of the initial permeability as a function of frequency of $\text{Ni}_{0.8}\text{Zn}_{0.2}\text{Fe}_2\text{O}_4$ sintered in different temperatures

Table 2: Magnetic properties of $\text{Ni}_{0.8}\text{Zn}_{0.2}\text{Fe}_2\text{O}_4$ sintered at different temperatures

Characterization	1100°C	1200°C	1300°C
Initial permeability at 10MHz	10	14	17
RLFx(10^{-5}) at 10MH	368	408	728
Grain size (μm)	0.201	0.280	0.326

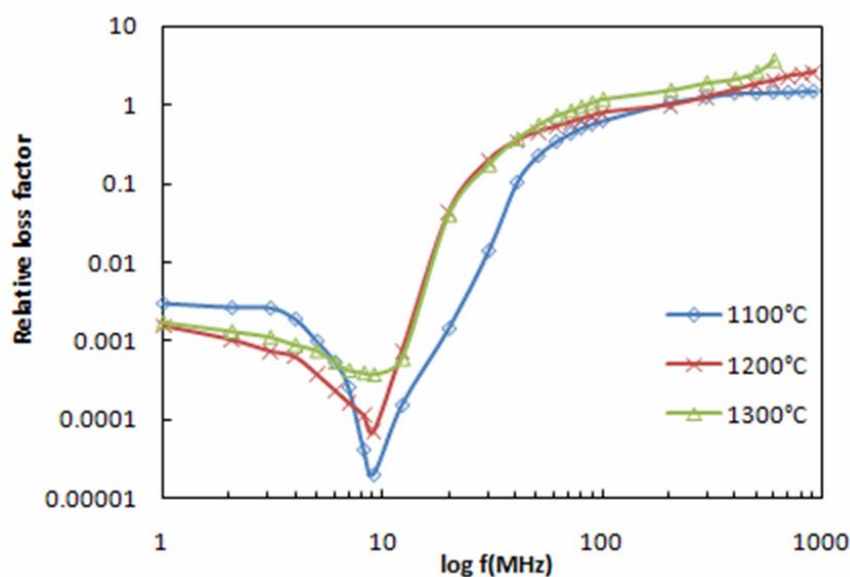


Figure 3: Variation of the RLF as a function of frequency of Ni_{0.8}Zn_{0.2}Fe₂O₄ sintered in different temperatures

The initial permeability, μ_i , as a function of frequency for the NiZn ferrite with the known composition in different temperatures is shown in Figure 2. The initial permeability values are lower than reported the those prepared via conventional technique. The permeability of polycrystalline ferrites is related to two different magnetization: spin rotation and domain wall motion. The contribution of spin rotation was found to be smaller than the domain wall movement [14,15].

The permeability is so sensitive to the microstructure such as porosity, grain size and pore distribution. Generally, the grain boundaries, local impurities and microstructural defects are relevant for pinning the domain wall. As tabulated in table 2, the initial permeability increases with sintering temperature. During sintering, the grain grows and larger grain tends to consist of a greater number of domain walls. As the number of walls increases with the grain size, the contribution of wall movement to magnetization increases. Hence, the initial permeability increased with higher sintering temperature . In the other words, the higher the density and larger grain size, the greater the grain- grain continuity in magnetic flux leading to higher permeability [15].

The energy losses versus a frequency are given in Figure3. The measured relative loss factor (RLF) is given in table 2. The loss can be written as $\alpha B + \beta f + \gamma$, where α and γ are the hysteresis and residual loss coefficients and β is the eddy current loss [16]. At lower frequency ,the loss factor is usually expressed by eddy current loss. Obviously, the RLF increases with sintering temperature. The larger grain increases the number and size of magnetic domains which contribute to loss due to delay in domain wall motion [16]. Thus, the larger grain increases the eddy current loss.

As shown in the Figure 3, the RLF decreases with the frequency from 1 MHz to 10 MHz then sharply increases. The relative loss factor values were observed to be of the order of 10^{-2} - 10^{-4} in the range of frequencies 1MHz to 10 MHz.

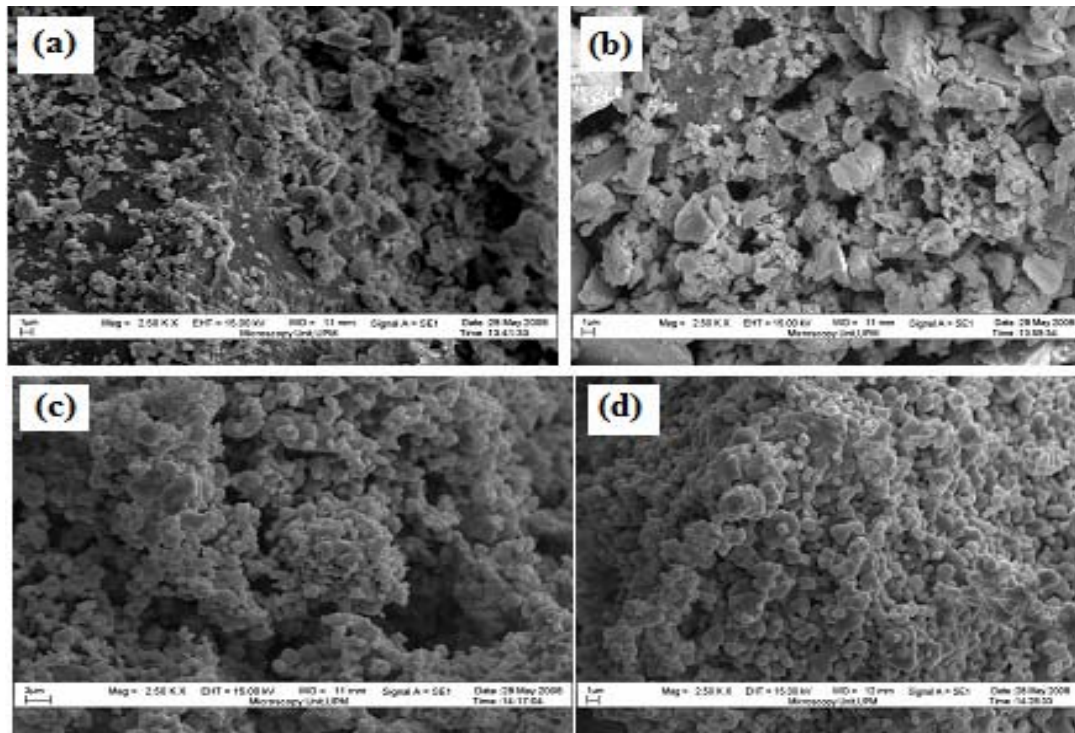


Figure 4: SEM photographs of NiZn ferrites in (b) 1100, (c) 1200, (d) 1300°C and (a) as dried sample

The morphology of the particles in the previous as-dried and calcined samples for 5 h is shown in Figure 4. Studies of scanning electron micrographs indicate that the grain size increases with increasing sintering temperature and time. In the present samples the grain size increases from the sample sintered at 1100°C to the sample sintered at 1300°C for 5 h. The grain size was measured from SEM micrographs, the average grain size was found to vary from 290 to 340 nm. It is also observed that the grains have an approximate spherical shape. The formation of the aggregated crystallites commenced at 1200°C. Uniform grains were observed at this temperature and their sizes were progressively increased at 1300 °C.

CONCLUSION

The present work suggests the magnetic behaviour of ferrites such as initial permeability and RLF prepared by co precipitation are better than those reported for NiZn ferrites prepared by the conventional method. The morphology studies indicated with homogeneity and high purity. The co precipitation is capable of giving smaller grains compared with those from the conventional methods. Therefore, the low RLF at 10 MHz is the advantage of this method. The simplicity and the lower sintering temperature and durations make this method preferable for producing better quality ferrites.

REFERENCES

- [1]. D.W. Johnson Jr., B.B. Ghate, in: F.F.Y. Wang (Ed.), 1985, *Proceedings of the Fourth International Conference on Ferrites, San Francisco*, October–November 1984, American Ceramic Society, Columbus, OH, p. 27.
- [2]. A.Goldman, in: C.M. Srivastava, M.J. Patni (Eds.), 1989, *Proceedings of the Fifth International Conference on Ferrites, Bombay*, Oxford and IBH, New Delhi, India, January p. 13.
- [3]. K.V.P.M. Shafi, A. Gedanken, R. Prozorov, J. Balogh, (1998), *J Chem. Mater.* **10** 3445.
- [4]. A. Hutlova, D. Niznanasky, J.L. Rehspringer, C. Estournes, M. Kurmoo, (2003), *Adv. Mater.* **15** 1622.
- [5]. C.T. Seip, E.E. Carpenter, C.J. O’Conner, J. Vijay, S. Li, (1998), *IEEE Trans. Magn.* **34** 1111.
- [6]. C. Pham-Huu, N. Keller, C. Estourne` s, G. Ehret, J.M. Grene` che, M.J. Ledoux, (2003), *Phys. Chem. Chem. Phys.* **5** 3716.
- [7]. Y.I. Kim, D. Kim, C.S. Lee, (2003), *Physica B* **337** 42.
- [8]. C. Liu, B. Zou, A.J. Rondinone, Z. Zhang, (2000), *J. Am. Chem. Soc.* **122** 6263.
- [9]. F. Li, J.J. Liu, D.G. Evans, X. Duan, (2004), *Chem. Mater.* **16** 1597.
- [10]. X.M. Liu, S.Y. Fu, C.J. Huang, (2005) *Mater. Sci. Eng. B* **121** 255.
- [11]. J.L.H. Chau, M.K. Hsu, C.C. Kao, (2006), *Mater. Lett.* **60** 947.
- [12]. H.M. Deng, J. Ding, Y. Shi, X.Y. Liu, J. Wang, (2001), *J. Mater. Sci.* **36** 3273.
- [13]. V. Blaskov, V. Petkov, (1996), *J. Magn. Magn. Mater.* **162** 331.
- [14]. A. Globus, P. Duplex, M. Guyot, (1968), *IEEE Trans. Magn.* **7** 617.
- [15]. A. Globus, P. Duplex, (1968), *J. Appl. Phys.* **39** 727.
- [16]. J.L. Snoek, (1948), *Physica* **14** 207.
- [17]. A. Verma, R. Chatterjee, (2006), *J. Magn. Magn. Mater.* **306** 313–320.
- [18]. S. Zahi, A.R. Daud, M. Hashim, (2007), *Materials Chemistry and Physics* **106** 452–456